

New AM-FM Analysis Methods for Retinal Image Characterization

Victor Murray*, Marios Pattichis* and Peter Soliz†

*University of New Mexico, Department of Electrical and Computer Engineering, Albuquerque, NM-87131

†VisionQuest Biomedical and University of Iowa, Department of Ophthalmology and Visual Sciences.

E-mails: vmurray@ieee.org, pattichis@ece.unm.edu, psoliz@visionquest-bio.com

Abstract—We develop new amplitude-modulated frequency-modulated (AM-FM) based methods to address some issues associated with the semantic gap between visual and mathematical features presented by retinal diseases such as age-related macular degeneration (AMD). Through the processing of simulated and real, clinical retinal images we gain an understanding of the effects of basic morphological characteristics of lesions associated with AMD. Through synthetic simulations, we discuss how histograms of the instantaneous amplitude and the instantaneous frequency magnitude, extracted from different scales, can be used to differentiate between images of different sizes and edge sharpness, while maintaining invariance with respect to rotations. We show that AM-FM features extracted from low and very-low frequency scales can clearly differentiate between retinal images containing Temporal Concentrated Drusen (TCD) and Geographic Atrophy (GA). Shape, size, distribution and edge sharpness are visual features used by ophthalmologists in identifying lesions such as drusen. We propose the use of new AM-FM derived features to quantitatively define these visual descriptions.

I. INTRODUCTION

Macular degeneration, a progressive eye condition, affects up to 15 million Americans and millions more worldwide [1]. In adults over 60, in the USA, age-related macular degeneration (AMD) is the first cause of severe vision loss and blindness. Even though AMD never causes total blindness by itself, it robs those affected of their sharp central vision and can dim contrast sensitivity and color perception. There are two types of AMD: ‘wet’ and ‘dry’. Although there is no cure for AMD, there are treatments for the ‘wet’ type but not for the ‘dry’ type.

A number of different methods applied to AMD image analysis worked directly with the intensity information of the images [2]–[6]. In such approaches, an illumination correction is often a pre-processing step [2], [3], [6]. Furthermore, decisions are based on thresholds applied to the intensity, that are adapted to the database.

In this paper, we develop multi-scale Amplitude-Modulation Frequency-Modulation (AM-FM) methods. The use of AM-FM methods allows us to extract detailed textured information in terms of the instantaneous amplitude (IA) and the instantaneous-frequency (IF) [7]–[10]. Here, we note that the instantaneous frequency (IF) captures geometric structures unaffected by illuminations and it is also invariant to rotations and translations. We assess the effectiveness of an AM-

FM based content-based image retrieval (CBIR) technique in identifying and retrieving retinal images with specified lesions. An earlier application of AM-FM methods to CBIR can be found in [11]. We investigate how AM-FM methods can be used for characterizing edges, distribution and shape of the drusen.

In section II we present some background information on the use of AM-FM methods. In section III we develop AM-FM methods that are specifically adapted for applications to retinal image analysis. Results are given in section IV. We provide a discussion in section V and concluding remarks in section VI.

II. BACKGROUND

We consider multi-scale AM-FM representations of digital images given by [10], [12]:

$$I(k_1, k_2) \simeq \sum_{n=1}^M a_n(k_1, k_2) \cos \varphi_n(k_1, k_2). \quad (1)$$

In (1), a digital image $I(\cdot)$ is a function of a vector of spatial coordinates (k_1, k_2) . A collection of M different scales are used to model essential image modulation structure. The amplitude functions $a_n(k_1, k_2)$ are always assumed to be positive. Non-stationary images are represented using AM-FM in terms of instantaneous amplitude and instantaneous phase functions given by $\varphi_n(k_1, k_2)$ (see for example [7]). The basic idea is to let the frequency-modulated (FM) components $\cos \varphi_n(k_1, k_2)$ capture fast-changing spatial variability in the image intensity. For each phase function $\varphi_n(k_1, k_2)$ we define the instantaneous frequency (IF) $\nabla \varphi_n(k_1, k_2)$ in terms of the gradient

$$\nabla \varphi_n(k_1, k_2) = \left(\frac{\partial \varphi_n}{\partial k_1}(k_1, k_2), \frac{\partial \varphi_n}{\partial k_2}(k_1, k_2) \right). \quad (2)$$

To estimate the instantaneous amplitude (IA), the instantaneous phase (IP) and the instantaneous frequency (IF), we can first compute the extended version of the 1D analytic signal [13]:

$$\hat{I}_{AS}(k_1, k_2) = I(k_1, k_2) + j\mathcal{H}_{2d}[I(k_1, k_2)], \quad (3)$$

where \mathcal{H}_{2d} denotes a two-dimensional extension of the one-dimensional Hilbert transform operator.

We can then estimate the IA and the IP using:

$$\hat{a}(k_1, k_2) = |\hat{I}_{AS}(k_1, k_2)| \quad (4)$$

and

$$\hat{\varphi}(k_1, k_2) = \arctan\left(\frac{\text{imag}(\hat{I}_{AS}(k_1, k_2))}{\text{real}(\hat{I}_{AS}(k_1, k_2))}\right). \quad (5)$$

For estimating the IF we use a variable spacing, local quadratic phase (VS-LQP) method [10], [12]. For VS-LQP we first compute

$$\hat{\varphi}_1(k_1, k_2) = \frac{1}{n_1} \arccos\left(\frac{\bar{I}_{AS}(k_1 + n_1, k_2) + \bar{I}_{AS}(k_1 - n_1, k_2)}{2\bar{I}_{AS}(k_1, k_2)}\right) \quad (6)$$

and

$$\hat{\varphi}_2(k_1, k_2) = \frac{1}{n_2} \arccos\left(\frac{\bar{I}_{AS}(k_1, k_2 + n_2) + \bar{I}_{AS}(k_1, k_2 - n_2)}{2\bar{I}_{AS}(k_1, k_2)}\right), \quad (7)$$

where $\bar{I}_{AS}(k_1, k_2) = \hat{I}_{AS}(k_1, k_2)/|\hat{I}_{AS}(k_1, k_2)|$, n_1 and n_2 represent variable displacements, from 1 to 4, through columns and rows, respectively. As discussed in [10], for low frequencies, for more accurate estimates, we select the IF estimates that yield the lowest arguments for the $\arccos(\cdot)$ functions of (6) and (7). For higher frequencies, we modulate the input image to baseband prior to AM-FM demodulation.

III. METHODS

A. Four-scale filterbank design

In order to isolate different AM-FM components from (1), we use a multi-scale filter-bank. Here, the basic idea is to isolate different AM-FM components over different bandpass filters (see [14] for details). Fig. 1 (a) depicts the frequency support of this filterbank. In this design (see [10], [12]) each bandpass filter has frequency support in only two quadrants of the frequency spectrum.

The filters were designed using an optimum min-max, equiripple approach. Passband ripple was set at 0.017dB and the stopband attenuation was set to 66.02dB. For all filters, the transition bandwidths were fixed to $\pi/10$.

In Fig. 1, filter 1 corresponds to a low pass filter (LPF) with frequency support in $[-\pi/16, \pi/16]$ for both the x and y directions. For all the other filters, the bigger the label number of the filter, the more compact the frequency support that it has. The filters in the highest frequencies (filters from 2 to 7 in Fig. 1), have a bandwidth of $\pi/2$ for both x and y directions. The bandwidth is decreased by a factor of 0.5 for each added scale. In Fig. 1 (b), we provide a closeup that shows the low frequency filters.

TABLE I
BANDPASS FILTERS USED FOR ESTIMATING AM-FM IN A FOUR-SCALE FILTERBANK.

	Scale	Bandpass filters
LPF	Lowpass filter	1
VL	Very low frequencies	20 - 25
L	Low frequencies	14 - 19
M	Medium frequencies	8 - 13
H	High frequencies	2 - 7

B. AM-FM analysis by scales

We estimate AM-FM components over different scales (set of frequency bandpass filters, see Table I, and also Fig. 1, for correspondence between scales and bandpass filters). For each AM-FM component we use dominant component analysis (DCA) over the corresponding frequency bands (LPF, VL, L, M and H from Table I). In DCA, at every pixel, we select the AM-FM estimates from the bandpass filter that gave the highest IA estimate.

From each scale, we use the histograms of both the instantaneous amplitude a_i and the magnitude of the instantaneous frequency ($\nabla\varphi_i$) given by $\|\nabla\varphi_i\|$ as image features.

We use histograms of IA and the magnitude of the IF, $\|\text{IF}\|$, to create a feature vector for characterizing the retinal image. Using histograms from different scales the AM-FM information extracted can be analyzed to find differences among the characteristics of the images. For example, a region containing soft drusen will have different estimates for IF than a region with hard drusen. Using these histograms, we can find if a certain frequency component that encodes a feature is present at the image.

C. CBIR for the AMD images

We present an AM-FM approach for content-based image retrieval (CBIR) for the AMD images. In this approach we use the histograms of the IA and $\|\text{IF}\|$ extracted from different scales to construct a feature vector for image retrieval.

We use principal component analysis (PCA) to reduce the numbers of bins in the histograms. We select the histogram projections that account for 95% of the covariance. With this new reduced feature vector from each image, we compute the distances among all the images using *correlation distance*:

$$d_{rs} = 1 - \frac{(x_r - \bar{x}_r)(x_s - \bar{x}_s)^T}{\left[(x_r - \bar{x}_r)(x_r - \bar{x}_r)^T\right]^{\frac{1}{2}} \left[(x_s - \bar{x}_s)(x_s - \bar{x}_s)^T\right]^{\frac{1}{2}}}, \quad (8)$$

where $\bar{x}_r = \frac{1}{n} \sum_j x_{rj}$ and $\bar{x}_s = \frac{1}{n} \sum_j x_{sj}$. With the computed distances between every single pair of images, we create a table of distances as shown in Table II. The retrieved images are then presented in ascending order using the computed distances from the query image.

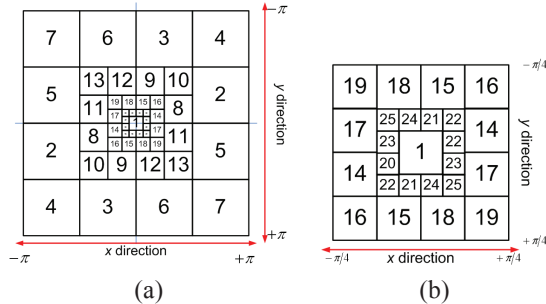


Fig. 1. Four-scale filterbank used for retinal image analysis. (a) Complete frequency spectrum of the filterbank. (b) Zoom on the low frequency bandpass filters.

TABLE II
DEFINITION OF THE TABLE OF DISTANCES.

	Image 1	Image 2
Image 2	distance{2,1}	
Image 3	distance{3,1}	distance{3,2}

IV. RESULTS

A. Synthetic Results

We use synthetic, elliptically-shaped images (see Fig.2) to investigate how differences in shape, size, orientation and edge sharpness influence the extracted AM-FM features. The AM-FM histograms are presented in Fig. 3.

We first present results when using ellipsoidal images of different sizes and the same blurring. In this experiment, we use synthetic examples from Figs. 2(a)-(e). Estimations used the entire filter-bank, yielding the histograms shown in Figs. 3 (a) and (b). In Table III we present the correlation distances using the histograms information for this example. Distances lower than 0.3 are highlighted.

In a second example, we investigate the effect on blurring, regardless of size. Here, we avoid using the LPF in our estimation, thus focusing on the fine edge details. For this example, we use the ellipsoidal images of Figs. 2 (c), (e)-(h). The resulting histograms are shown in Figs. 3 (c), (d). In Table IV, we show the correlation distances using the $\|IF\|$ histograms information for this example. The distances lower than 0.3 are highlighted.

For both examples, for estimating the histograms, we consider only the pixels that have an IA value bigger or equal than the global IA mean. Thus, our distances are based on the AM-FM values that gave the larger values.

B. Retinal Image Analysis

1) *A retinal image by scales*: We show an analysis by scales using AM-FM for an eye with Large Central Drusen (LCD) in Fig. 4. The original image is shown in Fig. 4 (a).

2) *A CBIR example*: We apply the method from sub-section IV-B2 to retrieve digital images with eyes containing Temporal Concentrated Drusen (TCD) and Geographic Atrophy (GA).

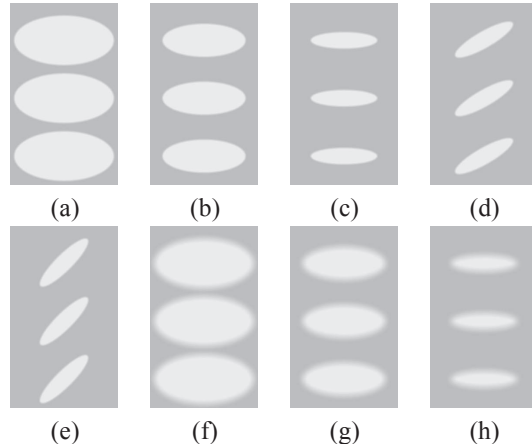


Fig. 2. Synthetic experiments using different shapes, sizes and edge sharpness: (a) large ellipses with major axis equal to 229 pixels and minor axis equal to 115 pixels, (b) medium ellipses with major axis equal to 193 pixels and minor axis equal to 77 pixels, (c) small ellipses with major axis equal to 155 pixels and minor axis equal to 39 pixels, (d) rotated small ellipse is the same as in (c) but rotated by 30° , (e) rotated small ellipse is the same as in (c) but rotated by 45° , (f) large ellipse is the same as in (a) but blurred with a 19×19 averaging filter, (g) medium ellipse is the same as in (b) but blurred with a 19×19 averaging filter and (h) small ellipse is the same as in (c) but blurred with a 19×19 averaging filter.

TABLE III
CORRELATION DISTANCES FOR SYNTHETIC SIMULATION EXAMPLES (SEE FIGS. 2 (A)-(E), FIGS. 3 (A)-(B)). WE USE LG TO DENOTE THE LARGE ELLIPSE, MD FOR THE MEDIUM, SM FOR SMALL AND ROT FOR ROTATED ELLIPSES. DISTANCES LOWER THAN 0.3 IN **BOLD** TYPEFACE.

	(a) LG	(b) MD	(c) SM	(d) ROT1 SM
(b) MD	0.118			
(c) SM	0.773	0.794		
(d) ROT1 SM	0.815	0.832	0.039	
(e) ROT2 SM	0.848	0.882	0.048	0.022

We use the green channel from the original color images. In Fig. 5, TCD images in (a)-(c) and GA images in (d)-(f).

We create the 64-bin histograms of IA and $\|IF\|$ for each image at the scales VL and L (see Table I). In Table V we show the correlation distances. The distances lower than 0.5 are highlighted. For all the histograms, we consider only the pixels that has an IA value bigger or equal than the 10% of the maximum IA value. PCA was used to select histogram

TABLE IV
CORRELATION DISTANCES FOR $\|IF\|$ FOR SYNTHETIC SIMULATION EXAMPLES (WITHOUT LPF). HERE, WE USE BL TO DESIGNATE AN IMAGE WITH BLURRY EDGES. DISTANCES LOWER THAN 0.3 IN **BOLD** TYPEFACE.

	(h) SM BL	(g) MD BL	(f) LG BL	(c) SM
(g) MD BL	0.116			
(f) LG BL	0.059	0.099		
(c) SM	0.603	0.330	0.595	
(e) ROT SM	0.518	0.435	0.530	0.275

TABLE V
CORRELATION DISTANCES IN THE CBIR EXAMPLE WHEN USING IMAGES FROM FIG. 5. DISTANCES LOWER THAN 0.5 IN BOLD TYPEFACE. (A)-(C) TCD IMAGES. (D)-(F) GA IMAGES.

	(a) TCD	(b) TCD	(c) TCD	(d) GA	(e) GA
(b) TCD	0.478				
(c) TCD	0.098	0.241			
(d) GA	1.784	1.340	1.845		
(e) GA	1.727	1.941	1.930	0.364	
(f) GA	1.583	1.968	1.852	0.461	0.018

projections that account for 95% of the covariance.

V. DISCUSSION

When comparing elliptic shapes with different sizes (see Figs. 2 (a)-(e)), using the entire filter-bank we are able to distinguish among different sizes. In the first example, from Table III, we can see how the distances for images with small ellipses are lower than 0.05 compared with the big and medium ellipses with distances bigger than 0.7.

In the second example, we can see that the instantaneous frequency magnitude can help us distinguish between blurred and non-blurred edges (see Table IV). Here, we can see that the distances among blurred ellipses are lower than 0.15 compared with those with no blurring, irrespective of the size of the ellipse.

From the synthetic examples, it is clear that the AM-FM estimates at different frequencies (or scales in this case) are able to characterize different visual features of the images. When using actual retinal images, we can see from Fig. 4 how the AM-FM features extract image characteristics at different scales. Here, we cannot see significant structural information in the “Medium” and “High” scales (see Figs. 4 (r)-(y)). On the other hand, it is clear that significant structural information can be extracted at the “Very Low” and “Low” scales. For example, at the “Very Low” scale, we note significant LCD features that are extracted by AM-FM features (see Figs. 4 (j)-(m)).

Based on these results, we use only the “Very Low” and “Low” scales for the CBIR application for our clinical example. We can see in Table II the big differences in the distances between images with TCD and images with GA. For images of the same group, the distances are lower than 0.5 whereas the distance between an image with TCD and an image with GA is always larger than 1.0.

VI. CONCLUSIONS

We have developed AM-FM methods for characterizing retinal images. We show that AM-FM feature histograms of the instantaneous amplitude and instantaneous frequency magnitude can be used to differentiate between different spatial sizes and edge sharpness. A four-scale filterbank was used for extracting relevant image structure for real images. In preliminary results, we show that good CBIR results can be obtained from considering AM-FM estimates from the

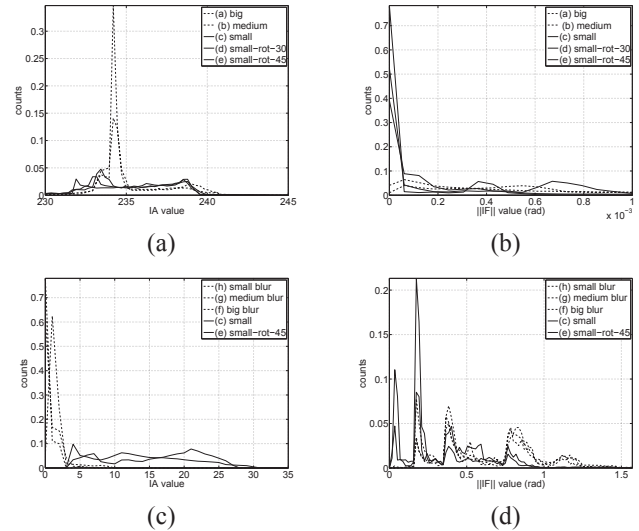


Fig. 3. IA and $\|IF\|$ histograms for synthetic simulation examples. (a) IA histograms using the entire filterbank, (b) $\|IF\|$ histograms using the entire filterbank, (c) IA histograms using the entire filterbank but without the LPF and (d) $\|IF\|$ histograms using the entire filterbank but without the LPF.

“Very Low” and “Low” scales. Shape, size, distribution and edge sharpness are visual features used by ophthalmologists in identifying lesions such as drusen. Visually these are referred to as soft or hard drusen, and distributed versus confluent drusen. Based on the preliminary results, we propose the use of new AM-FM derived features to quantitatively define these visual descriptions.

VII. ACKNOWLEDGEMENTS

The authors would like to thank Stephen R. Russell (M.D.) and Michael Abramoff (M.D., Ph.D.), from the Department of Ophthalmology & Visual Sciences at the University of Iowa, for selecting and grading the images for the studies that have made this research possible.

REFERENCES

- [1] The Macular Degeneration Partnership. [Online]. Available: <http://www.amd.org>
- [2] N. Lee, A. F. Laine, R. T. Smith, I. Barbazetto, and M. Busuico, “Quantification of geographic atrophy in fundus autofluorescence images for diagnosis of age-related macular degeneration,” *heffner Biomedical Imaging Lab*. [Online]. Available: http://hbil.bme.columbia.edu/wp-content/themes/HBIL_MJP/publications/156.pdf
- [3] R. Theodore Smith, J. K. Chan, T. Nagasaki, U. F. Ahmad, I. Barbazetto, J. Sparrow, M. Figueroa, and J. Merriam, “Automated detection of macular drusen using geometric background leveling and threshold selection,” *Arch Ophthalmol*, vol. 123, no. 2, pp. 200–206, 2005.
- [4] A. Mora, P. Vieira, and J. Fonseca, “Drusen deposits on retina images: Detection and modeling,” in *International Conference on Advances in Medical Signal and Information Processing*, 2004.
- [5] K. Rapantzikos and M. Zervakis, “Nonlinear enhancement and segmentation algorithm for the detection of age-related macular degeneration (AMD) in human eye’s retina,” in *IEEE International Conference on Image Processing*, vol. 3, 2001, pp. 1055–1058.
- [6] N. Lee, A. Laine, and R. Smith, “A hybrid segmentation approach for geographic atrophy in fundus auto-fluorescence images for diagnosis of age-related macular degeneration,” in *29th Annual International Conference of the IEEE Engineering in Medicine and Biology Society*, August 2007, pp. 4965–4968.

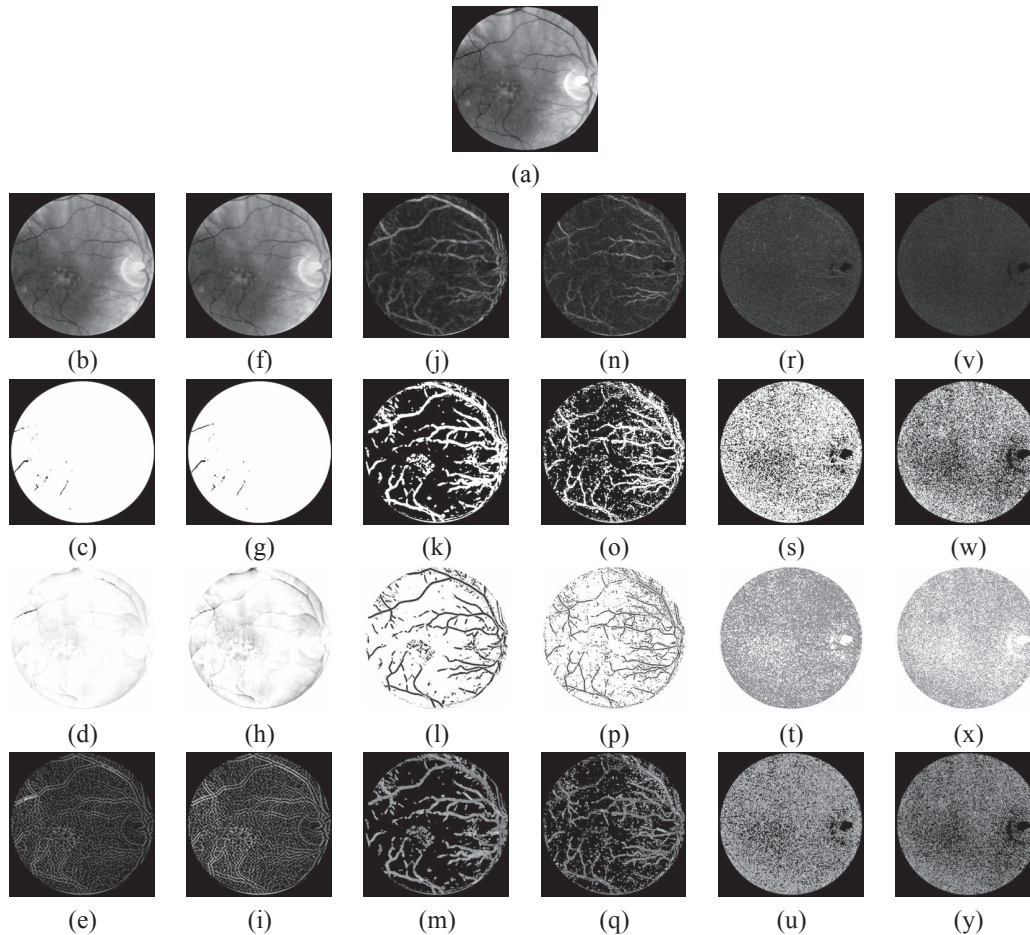


Fig. 4. AM-FM analysis of a retinal image with Large Central Drusen. For all AM-FM images in (b)-(y), we only show pixels where the IA is larger than 10% of the maximum IA value in the image. (a) Original image of size 1056×1056 , (b) AM-FM image ($a \cos \varphi$) reconstruction for all filters, (c) mask showing the pixel locations with IA bigger than 10% of the maximum IA value, (d) FM image ($\cos \varphi$) for all filters, (e) instantaneous frequency magnitude ($|\nabla \varphi_i|$) for all filters, (f)-(i) same as (b)-(e) for the LPF, (j)-(m) same as (b)-(e) for the very low frequency scale, (n)-(q) same as (b)-(e) for the low frequency scale, (r)-(u) same as (b)-(e) for the medium frequency scale, (v)-(y) for the high frequency scale.

- [7] M. S. Pattichis and A. C. Bovik, "Analyzing image structure by multidimensional frequency modulation," *IEEE Transactions on Pattern Analysis and Machine Intelligence*, vol. 29, no. 5, pp. 753–766, 2007.
- [8] J. P. Havlicek, D. S. Harding, and A. C. Bovik, "Multidimensional Quasi-Eigenfunction Approximations and multicomponent AM-FM models," *IEEE Transactions on Image Processing*, vol. 9, no. 2, pp. 227–242, February 2000.
- [9] M. Pattichis, C. Pattichis, M. Avraam, A. Bovik, and K. Kyriakou, "AM-FM texture segmentation in electron microscopic muscle imaging," *IEEE Transactions on Medical Imaging*, vol. 19, no. 12, pp. 1253–1258, December 2000.
- [10] Victor Manuel Murray Herrera, "AM-FM methods for image and video processing," Ph.D. dissertation, University of New Mexico, September 2008.
- [11] J. Havlicek, J. Tang, S. Acton, R. Antonucci, and F. Quandji, "Modulation domain texture retrieval for CBIR in digital libraries," in *37th IEEE Asilomar Conference on Signals, Systems and Computers*, Pacific Grove, CA, November 2003.
- [12] V. Murray, P. Rodriguez, and M. S. Pattichis, "Multi-scale AM-FM demodulation and reconstruction methods with improved accuracy," submitted to the *IEEE Transactions on Image Processing*, 2008.
- [13] J. P. Havlicek, "AM-FM image models," Ph.D. dissertation, The University of Texas at Austin, 1996. [Online]. Available: <http://hotnsour.ou.edu/joebob/PdfPubs/JPHavlicekDiss.pdf>
- [14] V. Murray, P. Rodriguez V., and M. S. Pattichis, "Robust multiscale AM-

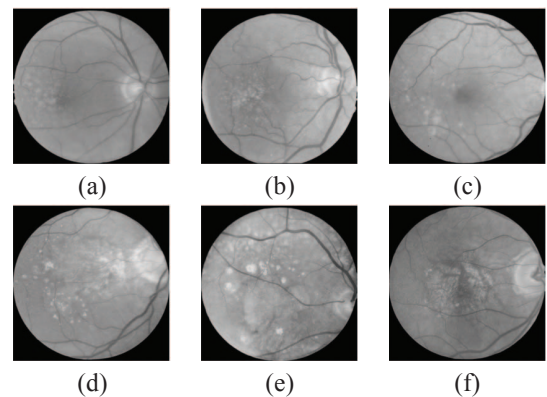


Fig. 5. Retinal images used for CBIR. (a)-(c) Images with Temporal Concentrated Drusen. (d)-(f) Images with Geographic Atrophy.

FM demodulation of digital images," in *IEEE International Conference on Image Processing*, vol. 1, October 2007, pp. 465–468.